We are IntechOpen,
the world's leading publisher of
Open Access books
Built by scientists, for scientists

6,900
Open access books available

186,000
International authors and editors

200M
Downloads

Our authors are among the

154
Countries delivered to

TOP 1%
most cited scientists

12.2%
Contributors from top 500 universities

CLARIVATE ANALYTICS
BOOK CITATION INDEX
INDEXED

WEB OF SCIENCE™

Selection of our books indexed in the Book Citation Index
in Web of Science™ Core Collection (BKCI)

Interested in publishing with us?
Contact book.department@intechopen.com

Investigation of Ground Remote Sensing Techniques for Supporting an Early Warning Water-Leakage System

Athos Agapiou, Dimitrios D. Alexakis,
Kyriacos Themistocleous, Apostolos Sarris,
Skevi Perdikou, Chris Clayton and
Diofantos G. Hadjimitsis

Additional information is available at the end of the chapter

1. Introduction

The decrease of water availability is a major global problem that is increasing in intensity. Since water resources have been substantially reduced over the past years, control over water distribution is now considered imperative. For this reason, water supply networks are more closely monitored and significant efforts are made to reduce the effects of leakages. In addition to the design and maintenance of water distribution systems, researchers are also focused on the improvement of early detection and rapid response of a leakage. Research indicates that water supply network may lose up to 20-30% of water, with the main cause being water leaks (Cheong, LC 1991). In some networks, the loss can reach more than 50% (AWWA, 1987).

Systematic leakages can lead to significant losses in both water as well as financial resources. Water pipe networks, regardless of age, often present problems of water leakage, resulting in large losses of precious drinking water. Therefore, there is an urgent need to design and build systems that can detect the presence and location of leaks in water pipes networks. The detection of hidden leaks in underground water supply networks requires the use of instruments designed specifically for this purpose by a trained operator.

The most widely applied technique for the detection of hidden leaks is the acoustic method. Additional methods for leak detection also include thermography, remote sensing, geophysics etc. Leaks from pipelines under pressure create a whistling characteristic noise, which is transmitted by the water itself. Hunaidi and Chu (1999) used the acoustic method for leakage detection, which focused on various types of leaks under controlled conditions. Hunaidi and

Giamou (1998) conducted a survey on the effectiveness of acoustic methods and the dynamics of alternative non-acoustic methods for leak detection in plastic pipes, using penetrating ground radar to assess the potential leakage. The survey was conducted in a specially constructed facility where different types of leaks could be simulated under controlled conditions. The facility had a 200m long tube made from PVC, 150mm diameter, which was buried in soft muddy soil to a depth 2.4m. The research was performed using a radar antenna with frequencies of 50, 100, 200, and 450 MHZ.

Pickerill and Malthus (1998) study of water leakage detection using airborne remote sensing data used the analysis of soil moisture and vegetation biomass based on thematic maps. The researchers were able to detect two leaks from the surrounding environment of the Aqueduct of the North West England. Huang and Fipps (2002) used an airborne thermal sensor, including GPS receiver, for leakage detection over irrigation canals and pipelines. The sensor was able to record surface temperature as digital values ranging from 0-255 (8 bit). Based on the data, 45 areas where identified as potential leakage sites. Each site was mapped using Geographical Information System of the area. From the 45 areas, 11 sites were examined in-situ, with a success rate of 91%. The other sites were specific channels with cracks that were likely sources of leaks. The study concluded that the thermal imaging method was a very promising technology for the evaluation of irrigation channels and leakage as it is a rapid and cost effective method of leak detection for irrigation channels. In a similar study, Huang and Fipps (2002) conducted a study in the Rio Grande Valley of Texas using airborne multispectral remote sensing for leak detection and possible identification of an irrigation network. A multispectral imaging system combining red, NIR and thermal sensors was used to collect image data in over 24 selected. During the flight, the three cameras (red, NIR and thermal) were synchronized to obtain the same area. Image processing included both image fusion as well as image geo-registration. The combination of red, NIR and thermal sensors were effective for the determination of leakage areas. The study found that airborne multispectral imaging can be used for assessing both the conditions of the channel as well for the detection of leaks in irrigation distribution networks.

Shih and Jordan (1993) examined soil moisture detection using Landsat satellite images. The methodology involved daily temperature data and soil moisture measurements recorded with ground-based observations. The results indicated that the percentage content of soil moisture was inversely proportional to the temperature at the soil surface. The thermal infrared (IR) data from Landsat band 6 was classified into four land use classes using GIS data. The four main categories were agriculture, irrigation, urban and forest-wetlands. The thermal data were also used to evaluate four soil moisture conditions (water, very wet, wet, dry) and were used in each of the four classes mentioned above. The integration of Landsat images using GIS can be used to assess regional soil moisture conditions which can be adapted to identify water leak detection. Naimullah (2009) used satellite images for pipeline leak detection, further to the classification of land use in Mempatih, Pahang, Malaysia. The objective of the study was the evaluation of vegetation indices such as NDVI images using SPOT-5 satellite data. The final results showed a correlation of 81.02% for NDVI to identify the leakage problem.

The research presented above, along with the studies discussed in this book, highlight the significant contribution of satellite imagery for the detection of leakages. In this chapter, further investigation of the use of ground remote sensing to identify water leakage in Cyprus is presented.

2. Methodology and resources

In the study of leakage detection in Cyprus, ground spectroradiometers and a digital infrared thermometer were the main tools used to monitor and investigate potential leakage events. In order to use ground spectroscopy for the detection of leakage problems, several measurements were made in a controlled environment. The experiment was conducted at the Agricultural Research Institute, located in Acheleia, Cyprus. The area of interest measured approximately 11 x 7 meter, as indicated in Figure 1. A grid of 1 x 1 meter was created to take measurements. Measurements were taken with a ground spectroradiometer before and after the flooding of the pipeline in order to compare the difference observed in the spectral signatures profiles. Due to weather conditions, frequent calibration of the incoming solar radiation using the Spectralon panel was necessary. The Spectralon panel is a Lambertian surface with 99.99% reflectance. Areas with shadows were excluded in this study in order to avoid misleading results. The measurements were taken on clean and dry ground.

Figure 1. Area of interest. A pipeline was buried at a depth of approximately 1 meter.

In this area, a pipeline was buried 1 meter below surface. Cracks were produced in the pipeline in order to create an artificial leakage event. The end of the pipeline was connected to a valve. Figure 2 shows the area of interest approximately one hour after the artificial leakage event.

Figure 2. Leakage as observed from the surface

The GER 1500 PC Graphing Application Software was used for the analysis of the measurements and to plot the spectral signatures. For the calculation of the vegetation indices, a Matlab code was applied. The maps were created using the ArcGIS software. Based on the Relative Response Filters of the Landsat 7 ETM+sensor, the narrow band reflectance recorded from the spectroradiometer was recalculated into the above satellite sensor. By using the broadband reflectance values (Bands 1 – 4; Blue / Green / Red / Near Infrared) several vegetation indices were calculated as shown in table 1.

no	Vegetation Index	Equation
1	EVI (Enhanced Vegetation Index)	$2.5 (p_{NIR} - p_{red})/(p_{NIR} + 6\, p_{red} - 7.5\, p_{blue} + 1)$
2	Green NDVI (Green Normalized Difference Vegetation Index)	$(p_{NIR} - p_{green})/(p_{NIR} + p_{green})$
3	NDVI (Normalized Difference Vegetation Index)	$p_{NIR} - p_{red}/(p_{NIR} + p_{red})$
4	SR (Simple Ratio)	p_{NIR}/p_{red}
5	MSR (Modified Simple Ratio)	$p_{red}/(p_{NIR}/p_{red} + 1)^{0.5}$

no	Vegetation Index	Equation
6	RDVI (Renormalized Difference Vegetation Index)	$(p_{NIR} - p_{red})/(p_{NIR} + p_{red})^{1/2}$
7	IRG (Red Green Ratio Index)	$p_{Red} - p_{green}$
8	RVI (Ratio Vegetation Index)	p_{red}/p_{NIR}
9	MSAVI (Modified Soil Adjusted Vegetation Index)	$[2 p_{NIR} + 1 - [(2 p_{NIR} + 1)^2 - 8(p_{NIR} - p_{red})]^{1/2}]/2$
10	ARVI (Atmospherically Resistant Vegetation Index)	$(p_{NIR} - p_{rb})/(p_{NIR} + p_{rb})$, $p_{rb} = p_{red} - \gamma (p_{blue} - p_{red})$
11	GEMI (Global Environment Monitoring Index)	$n(1 - 0.25n)(p_{red} - 0.125)/(1 - p_{red})$ $n = [2(p_{NIR}^2 - p_{red}^2) + 1.5 p_{NIR} + 0.5 p_{red}]/(p_{NIR} + p_{red} + 0.5)$
12	SARVI (Soil and Atmospherically Resistant Vegetation Index)	$(1 + 0.5)(p_{NIR} - p_{rb})/(p_{NIR} + p_{rb} + 0.5)$ $p_{rb} = p_{red} - \gamma (p_{blue} - p_{red})$
13	OSAVI (Optimized Soil Adjusted Vegetation Index)	$(p_{NIR} - p_{red})/(p_{NIR} + p_{red} + 0.16)$
14	DVI (Difference Vegetation Index)	$p_{NIR} - p_{red}$
15	SR × NDVI (Simple Ratio x Normalized Difference Vegetation Index)	$(p_{NIR}^2 - p_{red})/(p_{NIR} + p_{red}^2)$

Table 1. Vegetation indices used in this study.

A handheld digital infrared thermometer was also used to measure the ground temperature of the area. By using the laser sighting, measurements were taken at 1 meter intervals, before the leakage, during the leakage as well after the leakage event. Although the weather may have varied before, during and after the leakage, this had no impact on the results since the maps presented and discussed are based on relative differences in temperature. After the recording of the measurements, the ArcGIS was used to plot the data. Several interpolation methods were used, including the inverse distance to the power (IDW).

3. The use of UAV for detecting water leakages

Unmanned aerial vehicles (UAVs) have been used for monitoring purposes of leakages events in several semi-arid areas of Cyprus. Due to the low cost and high quality image provided, UAVs are increasingly being used for field work. Research indicates that aerial remote sensing

and imaging can be conducted using large scale low-altitude imagining and geospatial information (Colomina and Molina, 2014; Cho et al, 2013; Mayr, 2013; Petrie, 2013). In this study, a UAV platform was used to take aerial images of the study site. The UAV was equipped with RGB and VNIR cameras in order to document and detect water leakages from a low-altitude position. In this study, an octo-copter with 8 motorized propellers, including a GPS, piezo gyros, compass, altitude control, telemetry, acceleration and barometric sensor was used (figure 3.) The copter was used to take photographs of the water leakage events. Figure 4 features an aerial view of the Mandria water leakage site, while Figure 5 clearly shows the Lakatameia underground pipeline via aerial photography, with the continuation of the pipeline in yellow.

Figure 3. Oktocopter UAV

Figure 4. Leakage event in Mandria as observed from UAV

Figure 5. Lakatameia underground pipeline as observed from UAV

It was found that, in some cases, the UAV can identify water leakages and water pipelines in different ways such as increased vegetation along the pipeline where the water leakage occurs, change of soil characteristics along the pipeline route (Figure 5), as well as changes in the reflectance value of soils in the water leakage area. UAVs can also be used with thermal and infrared cameras to identify changes in temperature due to water leakage. An additional benefit of UAV platforms is that they can be used to survey large areas to provide overall coverage of the area or it can be used for areas that are inaccessible. The integration of UAV with other techniques is a useful method to cross-validate the leakage event.

4. Results

4.1. Digital Infrared Thermometer results

Figure 6 indicates the results from the ground temperature measurements before the leakage event. The results show that the minimum temperature values are recorded around the pipeline. This is most likely due to the presence of soil moisture resulting from a prior leakage, which occurred a month prior to the measurements. Similar results were also observed in the top of Figure 6, since the olive trees present in the area tend to hold moisture in the soil. In comparing the soil temperature over the pipeline against surrounding area, a relative differ-

ence of 2 °C was observed. This difference is logical, since from the last leakage event the soil temperature tends to be close to its original (background) value.
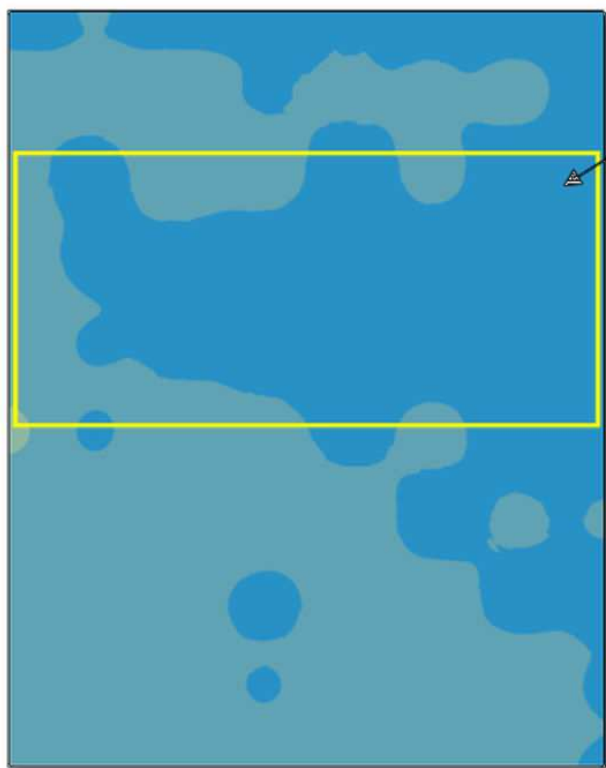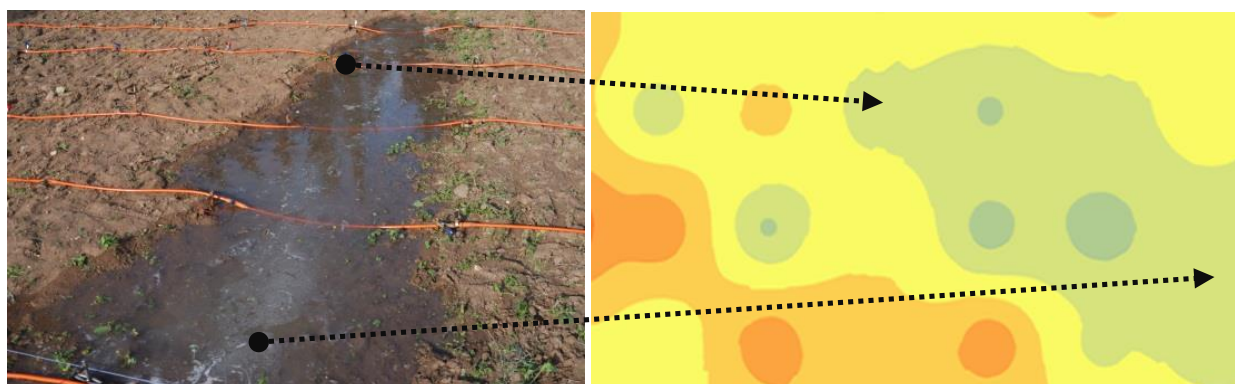

Figure 6. Ground temperature over the area of interest as recorded from the digital laser thermometer, before the leakage event. Rectangle indicates the location of the buried pipeline. Blue values indicates temperatures 14-16ᵒC while the cyan colour temperatures 16-18ᵒC.

Figure 7 demonstrates the results during the leakage event. The lowest surface temperature is shown in the western part area over the pipeline. In this section, the leak was initially observed during the leakage event. The soil temperature for the rest of the area was relatively high. These values indicate that moisture was not detected. The soil temperature also indicated a relative difference of about 6 °C of the leakage event and the rest dry area. Figure 8 features a photograph taken during the leakage event, as well the results from this area. The temperature measurements were able to map the problematic area with high accuracy and thereby define the leakage event. After the leakage event, the soil temperature decreased in the area over the buried pipeline. As shown in Figure 9, the entire pipeline had a tendency to present lower temperature values, including the leakage zone. The difference recorded in this step was estimate to be 8ᵒC.

In comparing the above figures, it appears that the soil temperature over the buried pipeline provided lower values before, during and after the leakage event. The relative temperature difference in this zone in relation to rest of the study area was initially small, then subsequently decreased and finally further decreased. The relative difference temperature of this zone prior to and after the leakage indicates a 60% reduction in relation to the surrounding area.
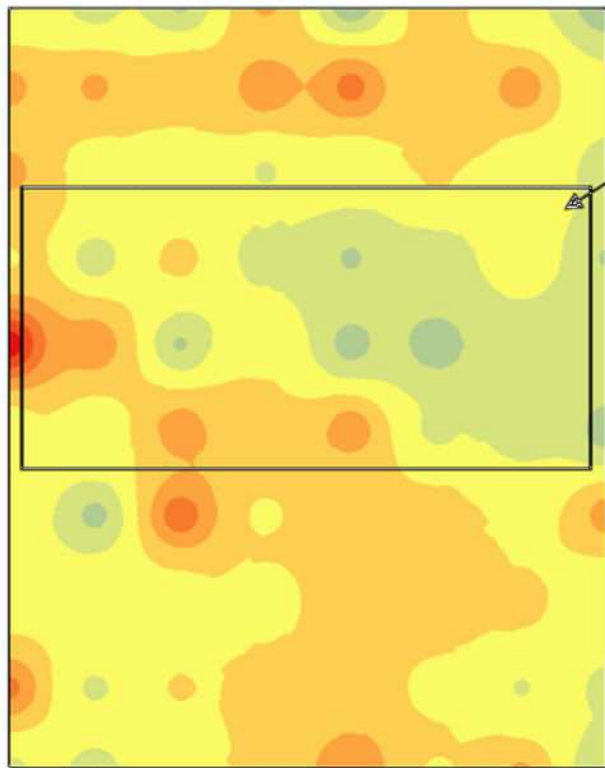
Figure 7. Ground temperature over the area of interest as recorded from the digital laser thermometer, during the leakage event. Rectangle indicates the location of the buried pipeline. Blue values indicates temperatures 14-16ºC, 24-26ºC are shown in yellow while orange colour highlight values from 34-36ºC


Figure 8. Detail of Figure 4. The lowest temperature values were recorded in the area were the leakage was still on going. The temperature map was able to draw with relative high precision the problematic area
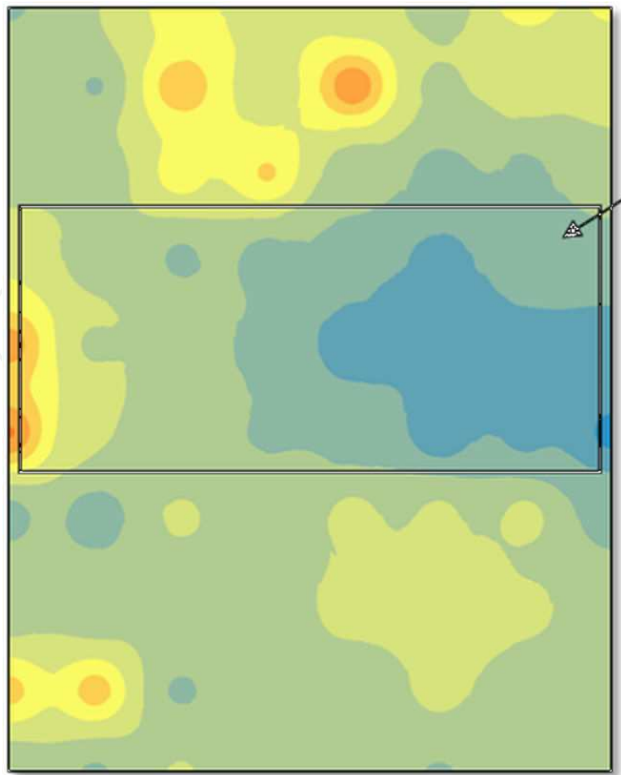
Figure 9. Ground temperature over the area of interest as recorded from the digital laser thermometer, during the leakage event. Rectangle indicates the location of the buried pipeline. Blue values indicates temperatures 14-16°C, 24-26°C are shown in yellow while orange colour highlight values from 34-36°C

4.2. Spectral signatures profiles

Figure 10 features the spectral signatures profiles from some regions of the study area before and after the leakage event. Using this figure, some preliminary conclusions can be drawn in relation with the reflectivity values of the same regions prior and after the leakage. The near infrared part of the spectrum (Band 4) tends to give the highest deviations. The reflectance values after the leakage is lower than prior to the event. Regarding the measurements over the pipeline there is a difference in the reflectance values before and after the leakage (spectral signature red and yellow).

4.3. Vegetation indices

Several vegetation indices were used in this study as shown in Table 1. Fifteen different broadband indices were calculated based on the RSR filters of Landsat 7 ETM+and applied in the area of interest. Some indices tended to provide poor results in contrast to other indices, which were able to detect the leakage. Several figures were created showing the area prior and after the leakage, as well maps showing the vegetation index difference.

As indicated in Figure 11, the EVI index was able to detect the leakage occurred over the buried pipeline with great success. As shown in figure 11, the highest negative values (blue colour)
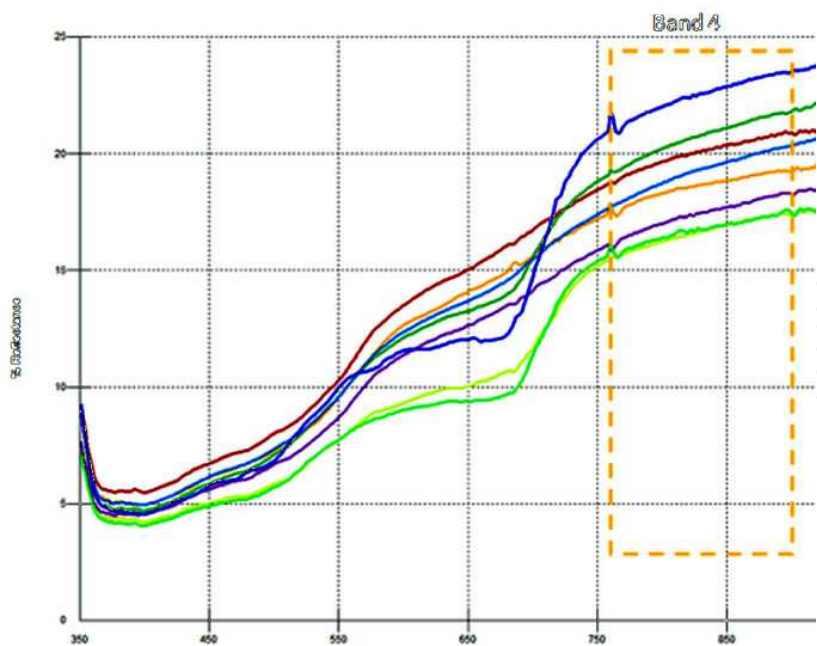
Figure 10. Spectral signatures profiles before and after the leakage event. The differences are maximized in the near infrared part of the spectrum (Band 4)

are observed in the area over the pipeline. In order to create this map, the EVI index was calculated before and after the leakage event and then these two indexes were subtracted. In a similar manner, the RDVI index was also able to show this leakage. A cross section from North to South was performed to see the vertical profile of the index. As demonstrated in Figure 12, the highest difference is recorded as the section pass through the pipeline (points A and B in Figure 12).

Several vegetation indices presented in Figures 13-25 were able to highlight the leakage as well as the area around the buried pipeline before and after the leakage (table 2). The buried pipeline is indicted by the black triangle in each figure. However, in addition to the leakage event, there were other parameters that played a significant role for the detection of the problem. As the results indicate, vegetation indices, including the NDVI index, were able to identify the leakage, yet there were some problems related to the atmospheric conditions. In contrast, the ARVI index was able to map the leakage with no difficulties since it is an atmospheric resistance index. EVI was another index with can be applied for this purposes as well.

Figure	Vegetation indice used
Figure 13	SRxNDVI
Figure 14	SR
Figure 15	Sarvi

| Figure	Vegetation indice used
Figure 16	RVI
Figure 17	OSAVI
Figure 18	NDVI
Figure 19	MSR
Figure 20	MSAVI
Figure 21	IRG
Figure 22	GNDVI
Figure 23	GEMI
Figure 24	DVI
Figure 25	ARVI

Table 2. Vegetation indices used in this study, by figure
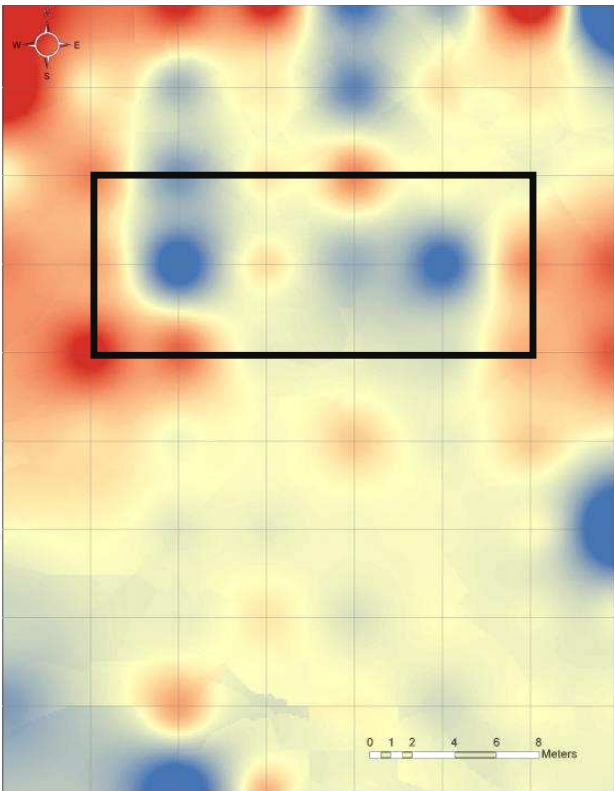
Figure 11. Difference values as calculated for EVI index (before and after the leakage). The buried pipeline is indicated in the rectangle.
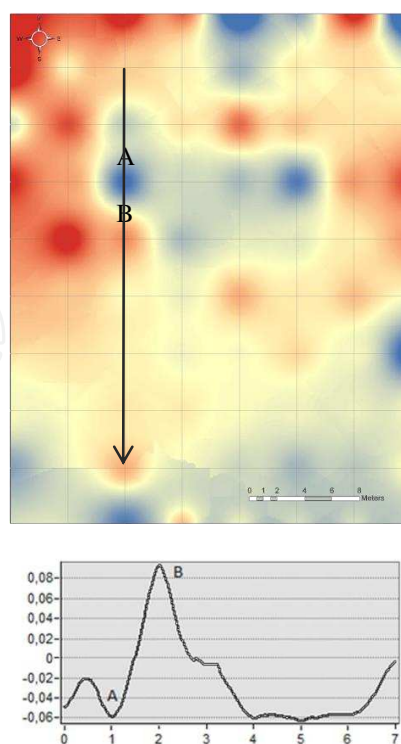
Figure 12. Difference values as calculated for RDVI index (before and after the leakage). A cross section passing through the pipeline (A-B) is also drawn.
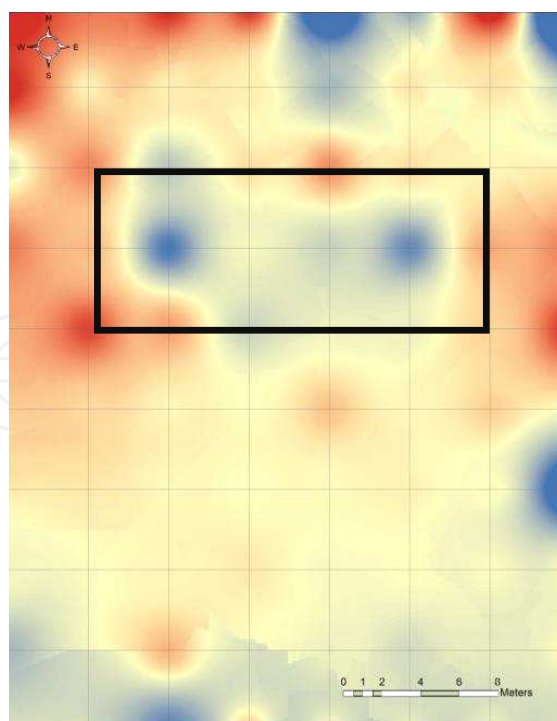
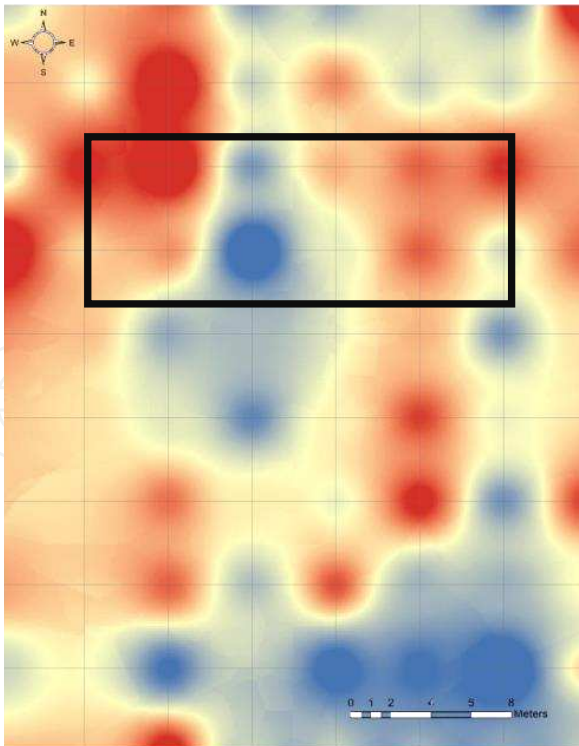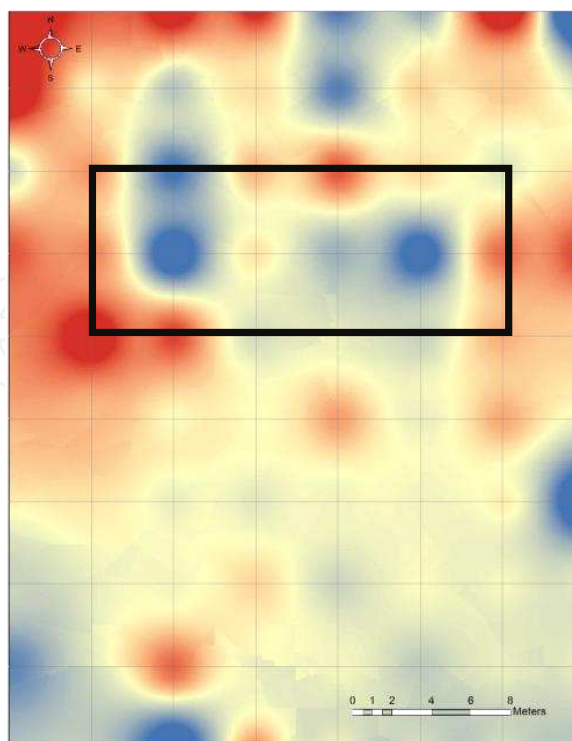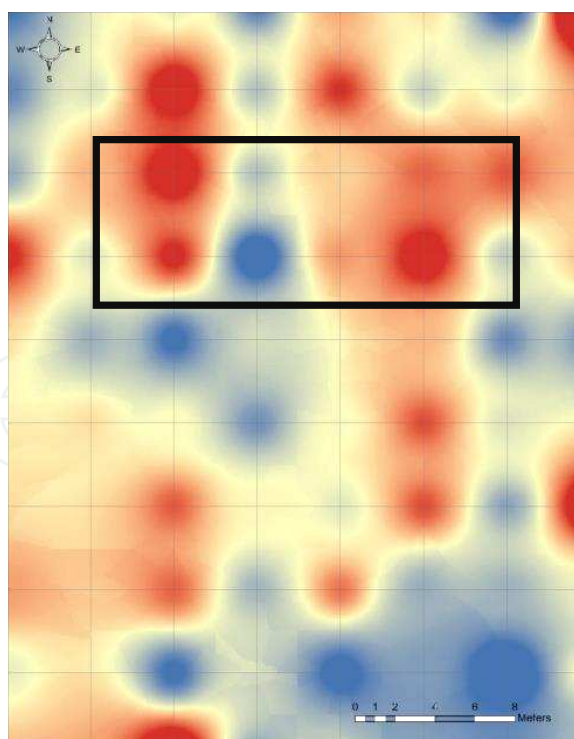**Figure 13.** Difference values as calculated for SRxNDVI index
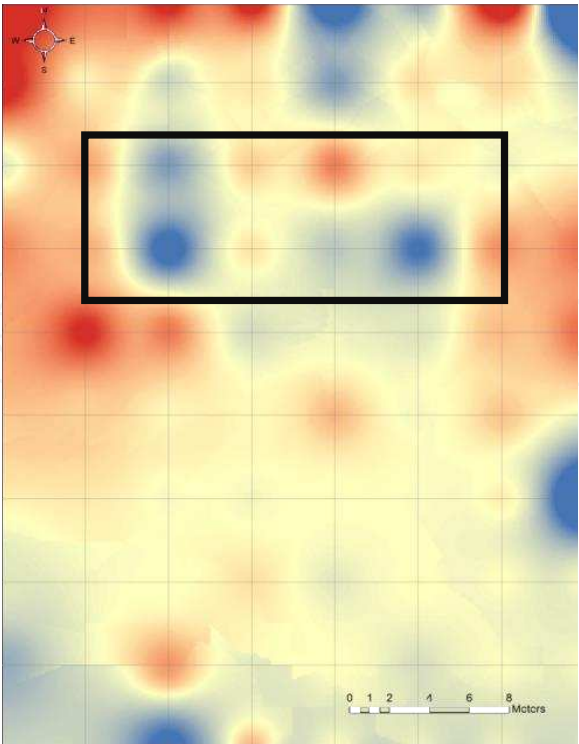
Figure 14. Difference values as calculated for SR index
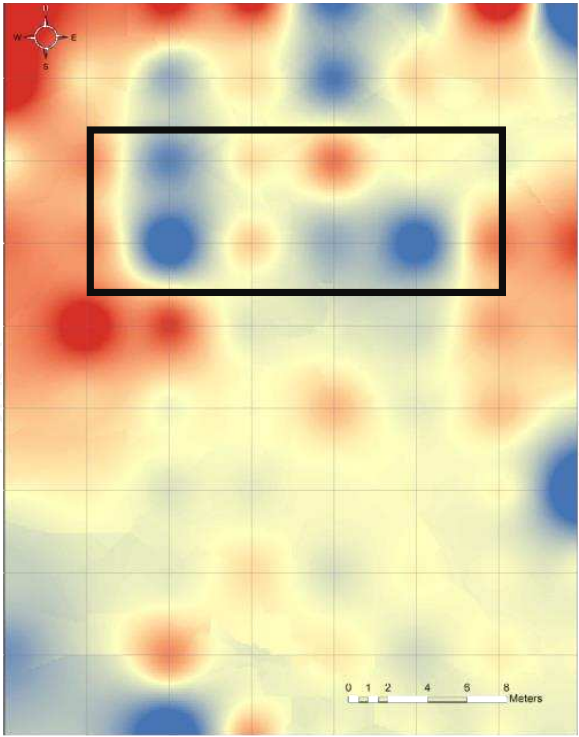
Figure 15. Difference values as calculated for SARVI index
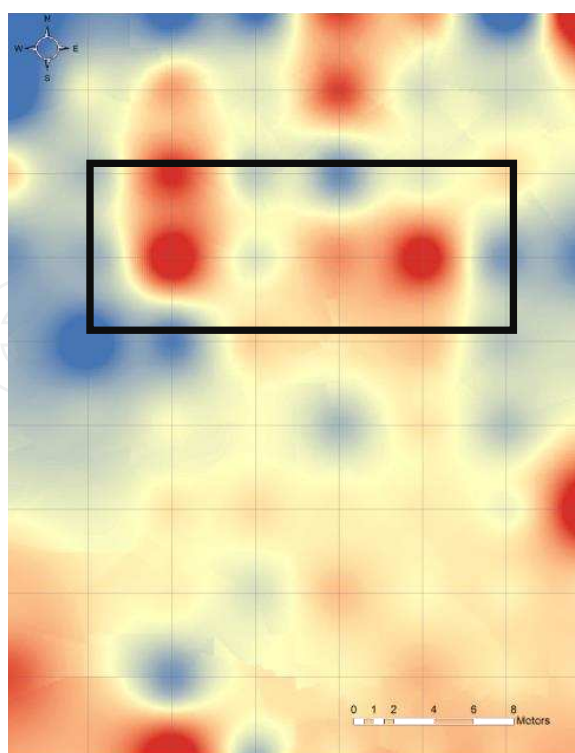
Figure 16. Difference values as calculated for RVI index
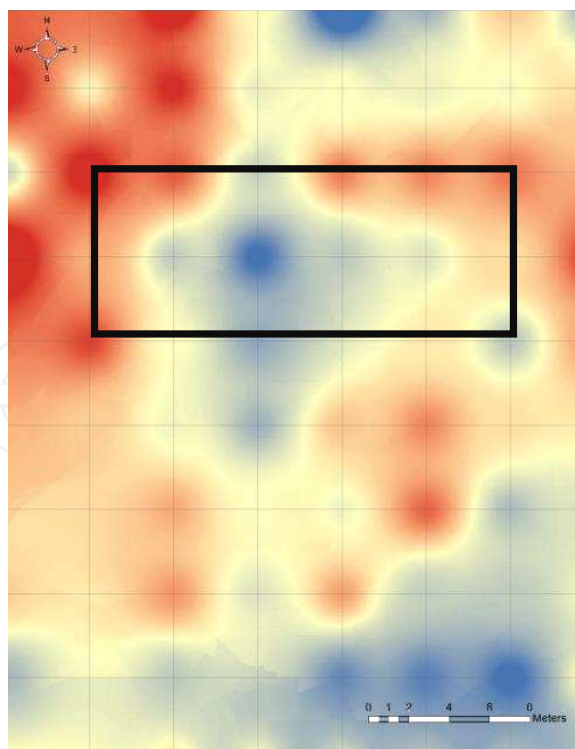
Figure 17. Difference values as calculated for OSAVI index
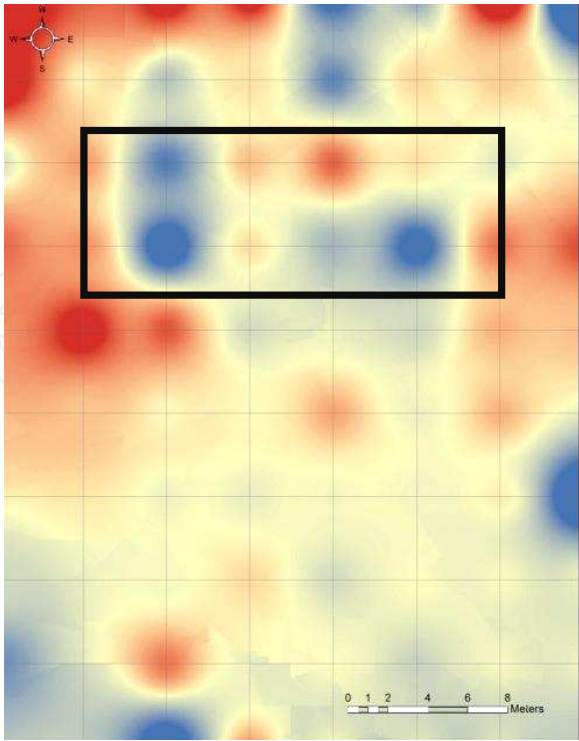
Figure 18. Difference values as calculated for NDVI index

Figure 19. Difference values as calculated for MSR index

Figure 20. Difference values as calculated for MSAVI index

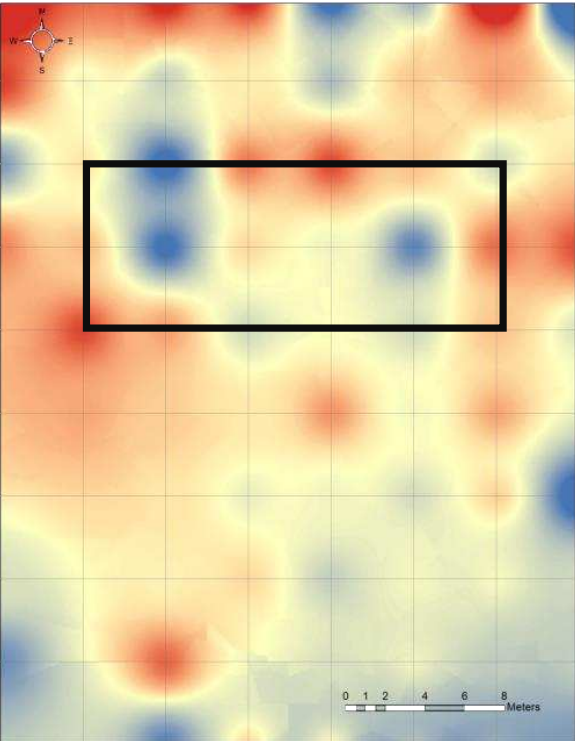**Figure 21.** Difference values as calculated for IRG index

Figure 22. Difference values as calculated for GNDVI index
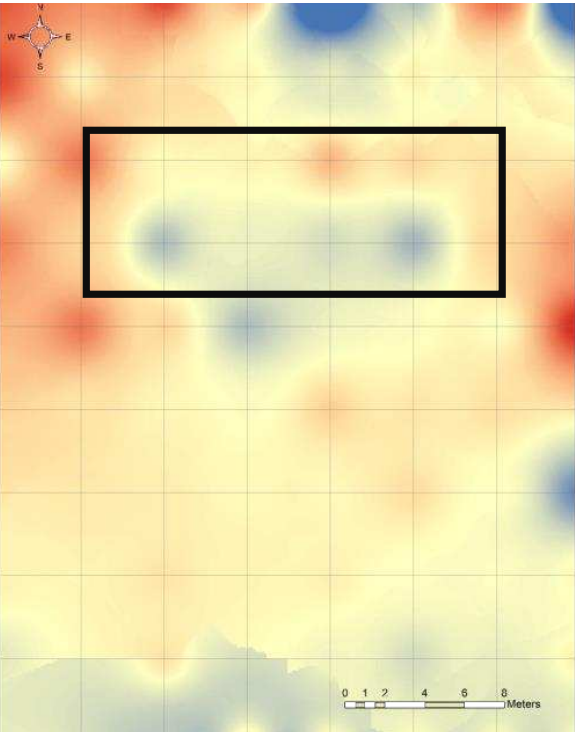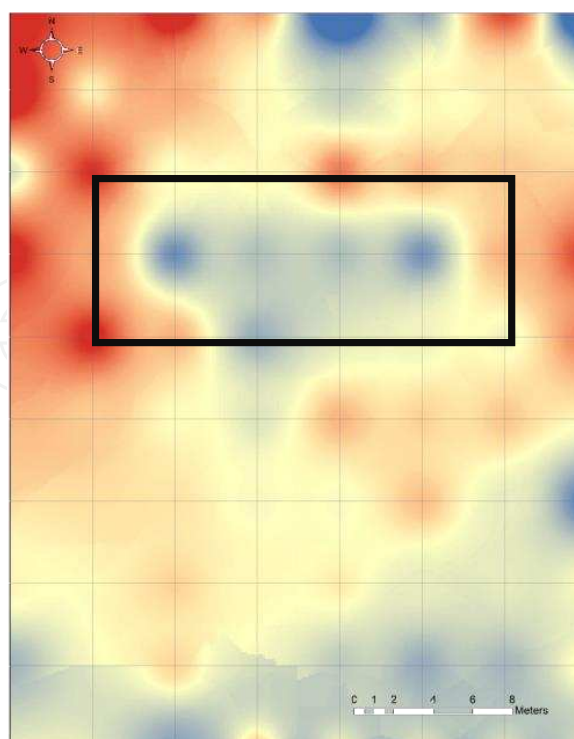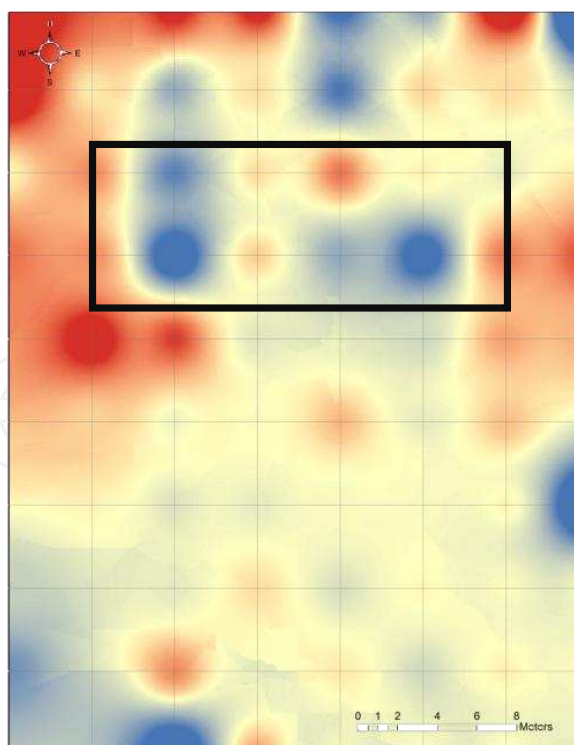

Figure 23. Difference values as calculated for GEMI index

Figure 24. Difference values as calculated for DVI index

Figure 25. Difference values as calculated for ARVI index

5. Development of a leakage early warning system

During the study, a methodology was developed for the local authorities and other end users regarding the early warning system. The early warning system was based on the study by Agapiou et al. (2014) and from the results of this controlled experiment. The system was built in the ArcGIS software with the objective to extract useful information from remote sensing satellite images. The methodology applied is divided into two different scenarios according to the amount of satellite images available to end users (see Figure 26).
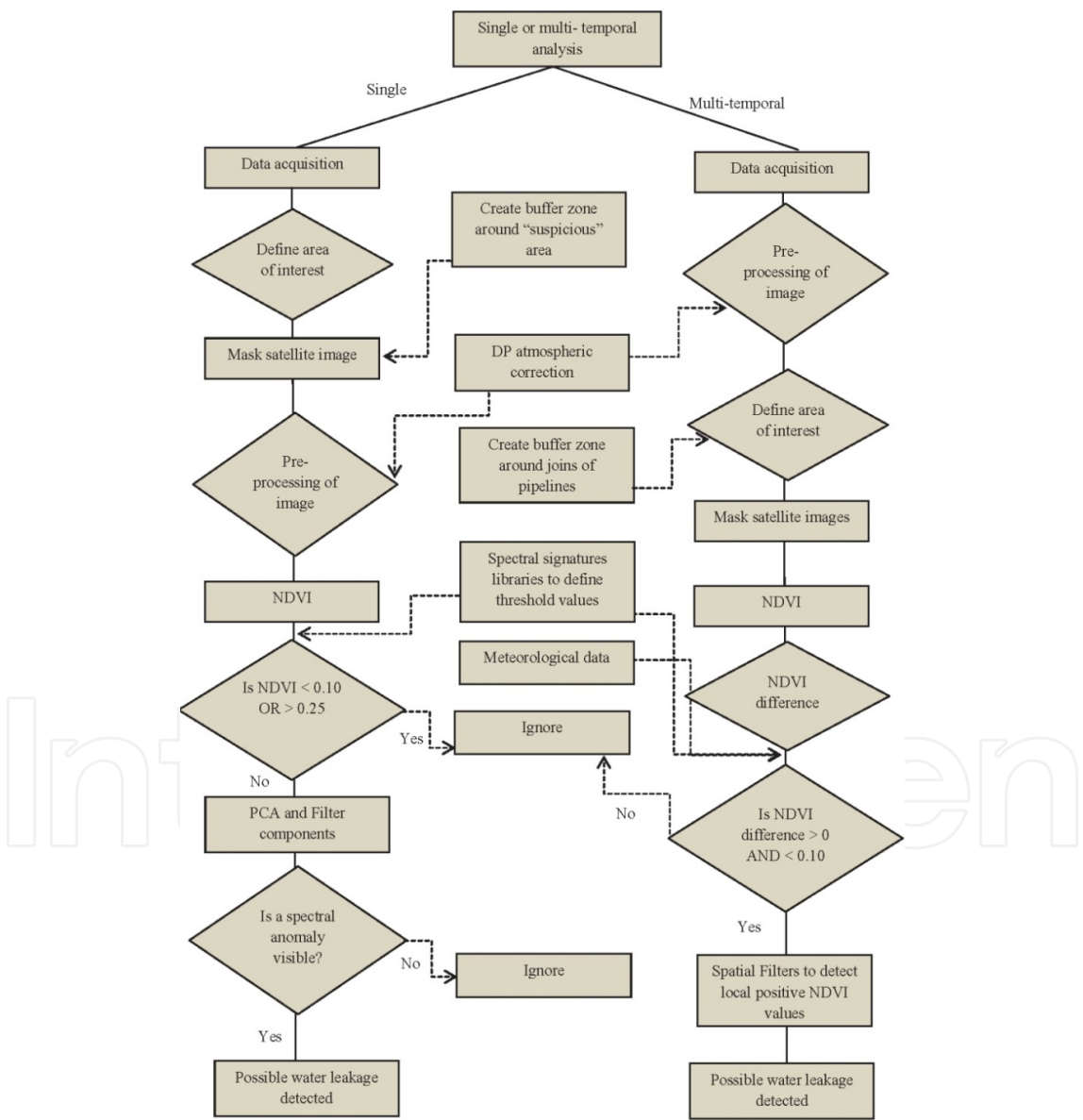

Figure 26. Methodology followed for the early warning system (Agapiou et al. 2014).

Figure 27. Detection of leakage problem using high resolution satellite data (Agapiou et al. 2014)

The first scenario aims to detect "suspicious areas" and therefore validate a hypothesis of a water-leakage event while the second scenario aims to detect unknown leakages events.

The first scenario is briefly outlined by the next steps:

Define the broader zone of "suspicious" leakages areas

Radiometric and Geometric corrections of the image, including atmospheric correction. In this study, the Darkest Pixel image based algorithm was applied since is a fast and accurate method for removing atmospheric effects

Calculation of the NDVI index in the area of interest

Definition of thresholds for the NDVI values. These thresholds were defined a-priori after field spectroradiometric campaigns

Masking of areas within thresholds boundaries

Application of other vegetation indices and PCA analysis as well as spatial filters for the detection of vegetated areas

Definition of areas with possible leakage problem

For the second scenario the steps are:

Radiometric and Geometric corrections of the images

Creation of buffer zones around the joints of the water pipeline

Masking of images

Calculation of NDVI index in the area of interest in the whole dataset

Calculation of NDVI difference between the two images

Definition of thresholds for the NDVI values based on pre-defined thresholds.

Definition of areas with possible leakage problems using spatial filters

The modeler was built into the ArcGIS environment and successfully applied using several satellite data. Previous studies of the authors (Agapiou et al. 2014) the detection of leakage events was possible (see Figure 27).

6. Discussion

Leakage detection is very important for water management. As presented in this chapter, research has indicated that remote sensing techniques can identify leakage detection. Remote sensing techniques can provide useful data, both for the detection of the water pipes and for the detection of water leakages. This study was conducted in a controlled environment using ground remote sensing techniques. The use of ground spectroradiometers has shown that several broadband vegetation indices may be applied for the detection of leakages events. The different maps created in this chapter indicate that some indices such as ARVI or EVI are favourable for this purpose. The results demonstrated that digital thermometers may be used for the detection of leakages events. Therefore, either airborne or satellite systems equipped with thermal sensors and with a high resolution may be possible detect areas with leakage problems. As well, UAVs can be used successfully to identify water leakages, through the use of aerial photography and other sensors. The results of this study indicate that remote sensing techniques are able to detect areas of the pipeline with water leakages. The resulting data can be integrated into a GIS which can be used by local authorities as an early warning system.

Acknowledgements

Author details

Athos Agapiou[1*], Dimitrios D. Alexakis[1], Kyriacos Themistocleous[1], Apostolos Sarris[2], Skevi Perdikou[3], Chris Clayton[4] and Diofantos G. Hadjimitsis[1]

*Address all correspondence to: athos.agapiou@cut.ac.cy

1 Department of Civil Engineering and Geomatics, Faculty of Engineering and Technology, Cyprus University of Technology, Cyprus

2 Laboratory of Geophysical - Satellite Remote Sensing & Archaeo-environment (GeoSat ReseArch), Institute for Mediterranean Studies (I.M.S), Foundation for Research & Technology, Hellas (F.O.R.T.H.), Crete, Greece

3 Department of Civil Engineering and Geomatics, Faculty of Civil Engineering, Frederick University, Cyprus

4 University of Southampton, School of Engineering and the Environment, UK

References

[1] Agapiou, A., Alexakis, D.D., Themistocleous, K. and Hadjimitsis. Water leakages detection using remote sensing, field specstroscopy and GIS in semiarid areas of Cyprus. *Urban Water Journal*, In press.

[2] AWWA. *Leaks in Water Distribution Systems – A Technical/Economic Overview*. Denver, Colorado: American Water Works Assoication. 1987.

[3] Cheong, L.C.. Unaccounted-for Water and the Economics of leak detection, in:Water Supply (eds.). *Proceedings of the International Water Supply Congress and Exhibition*. Copenhagen. Copenhagen: Water Supply. 1991. 1-6.

[4] Cho, G., (et al.) 2013. Pilotless aerial vehicle systems: size, scale and functions. *Coordinates*, 9, pp.8-16.

[5] Colomina, I. and Molina, P. 2014. Unmanned aerial systems for photogrammetry and remote sensing: a review. *ISPRS Journal of Photogrammetry and Remote Sensing*, 92, pp. 79-97.

[6] Huang, Y and Fipps, G. *Thermal Imaging of Canals for Remote Detection of Leaks: Evaluation in the United Irrigation District*-Technical Report. A&M University Texas: Biological and Agricultural Enginnering Department. 2002.

[7] Hunaidi, O. and Chu, W.T.. Acoustical characteritsics of leak signals in plastic water distribution pipes. *Applied Acoustics*, 1999. 58(235-254)

[8] Hunaidi, O and Giamou, P.. Ground Penetrating Radar for detection of leaks in buried plastic water distribution pipes, in:*Proceedings of the Seventh International Conference on ground Penetrating Radar*. Lawrence, Kansas. Lawrence, Kansas: 1998. 27-30.

[9] Mayr, W., 2013. Unmanned aerial systems-for the rest of us. Proc. 53rd Photogrammetric Week. Institute fur Photogrammetrie, Universitat Stuttgart, pp.125-134, (2013).

[10] Petrie, G., 2013. Commercial operation of lightweight UAVs for aerial imaging and mapping. GEOInformatics, 16, pp.28-39.

[11] Pickerill, J.M. and Malthus, T.J.. Leak Detection from Rural Aqueducts using Airborne Remote Sensing Techniques. *International Journal of Remote Sensing*, 1998. 19(12): pp. 2427-2433.

[12] Shih, S.F. and Jordan, J.D.. Use of Landsat Thermal-IR data and GIS in soil moisture assessment. *Journal of Irrigation and Drainage Engineering*, 1993. 119(5): pp. 868-879.